International Journal of Soft Computing 13 (6): 158-166, 2018
ISSN: 1816-9503

Speed Control of 8/6 Switched Reluctance Motor Using Torque Ripple Reduction Techniques

[1]Amged El Wakeel, [1]Usama Abou Zayed, [2]Mohamed E. Metally and [1]Ahmad Turk
[1]Department of Electrical Power and Energy Military Technical College, Cairo, Egypt
[2]High Institute of Engineering, El Shorouk Academy, Cairo, Egypt

Abstract: Switched Reluctance Motor (SRM) has become popular in various applications because of its high torque to inertia ratio, high efficiency, variable speed operation capabilities. The SRM primary drawback is torque ripples in the developed torque leading to notable noise and vibrations. Large torque ripples in SRM are due to the switching currents into its stator coils and its nonlinear magnetic nature during operation. By controlling and monitoring the torque of the SRM a significant decrease in torque ripples and even motor efficiency improvement can be carried out. In this study, two stochastic-based optimal PI controllers are used for speed control of an 8/6 SRM Model using MATLAB/Simulink tool with three types of torque sharing functions for torque ripple reduction and achieving overall performance improvement.

Key words: Switched Reluctance Motor (SRM), Firefly Algorithm (FA), Particle Swarm Optimization (PSO), torque ripples reduction, Torque Sharing Function (TSF), significant

INTRODUCTION

The SRM non-linear characteristics are the main reasons of torque ripples which are more intense than these of other commonly known electrical motors. If every single phase current can be controlled then the key issue is the selection of adequate current profiles to ensure low torque ripples. Also, torque produced by each phase should be arranged, so that, the total developed torque follows the reference value generated by the position or speed controllers. However, there is no unique distribution of torque between phases, so an efficient torque distribution scheme is needed. The developed torque entirely relies on the torque-current-angle characteristics of the motor. Furthermore, torque production is highly dependent on rotor position due to the absence of reference frame transformation for SRM.

Torque ripples reduction can be achieved by using different control techniques. The control approach depends on optimization of control parameters, including the voltage source, switching angles and current levels. Reduced noise and torque ripples and even efficiency improvement can be achieved by proper torque control of the SRM.

In this study, a PI speed controller is used with 3 different Torque Sharing Functions (TSF) to study thier impact on the performance of SRM and torque ripples reduction in particular. MATLAB/Simulink Software is used for simulation and analysis of the 8/6 SRM under study. The controller gains are optimized using Particle Swarm Optimization (PSO) and Firefly Algorithm (FA). A comparative study between the influence of the proposed control techniques on the system performance has been presented and discussed.

MATERIALS AND METHODS

System modeling

SRM modeling: The Simulink Model of the 8/6 SRM under study with its drive is shown in Fig. 1 and Table 1 (El-Wakeel, 2003; Torrey *et al*., 1995).

The SRM has a very high torque ripple component which is due to the current transition between consecutive phases. This torque ripple component which is a significant characteristic of the SRM mainly depends on the converter switching angles. The equations which govern the behaviour of the SRM drive can be written in the following form: (El-Wakeel, 2003; Miller, 2001; Krishnan, 2001). The electrical system:

$$V = R_s i + L(\theta,i)\frac{di}{dt} + \frac{dL(\theta,i)}{d\theta}\cdot\omega_m i \quad (1)$$

And:

$$T_e(\theta,i) = \frac{1}{2} i^2 \frac{dL(\theta,i)}{d\theta} \quad (2)$$

The mechanical system:

$$T_e(\theta,i) - T_l = J\frac{\omega_m}{dt} + B\omega_m \quad (3)$$

Corresponding Author: Amged El Wakeel, Department of Electrical Power and Energy, Military Technical College, Cairo, Egypt

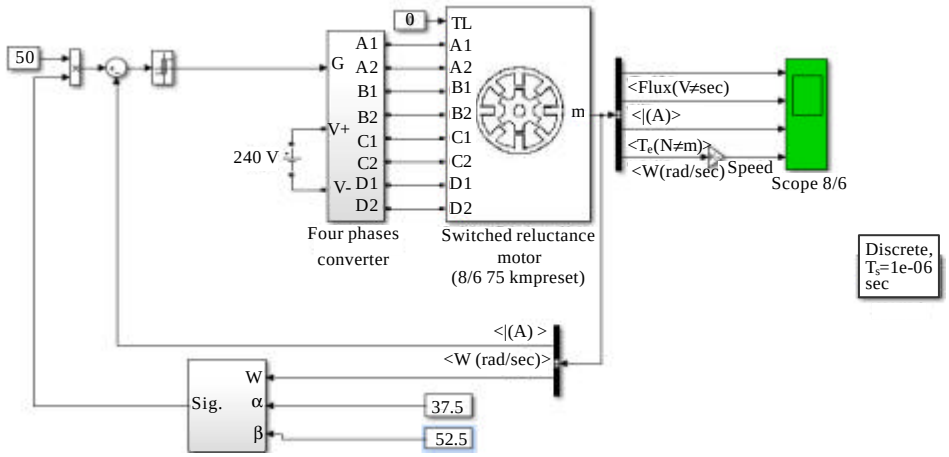

Fig. 1: Simulink model of a 8/6 SRM with its drive

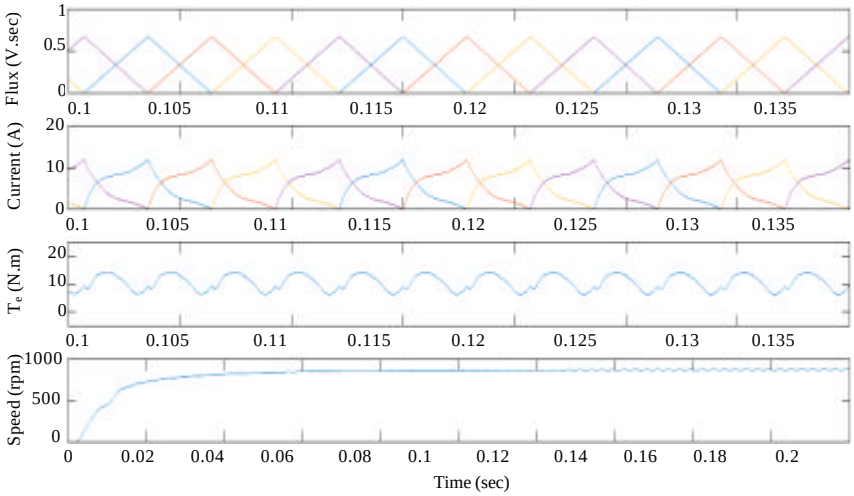

Fig. 2: Performance of 8/6 SRM operating with fixed switching angles

Table 1: 7.5kW, 8/6 SRM data

Variables	Values
Number of stator poles (M)	8 poles
Number of rotor poles (N)	6 poles
Supply voltage (V)	280 (V)
Peak phase current (I)	36.5 A
Phase resistance (R_s)	0.02 Ω
Inertia (J)	0.082 (kg. m^2)
Friction coefficient (B)	0.03 (N.m.sec)
Rated speed (n)	1500 (rpm)
Max. inductance (L_{max})	145.9 (mH)
Min. inductance (L_{min})	9.15 (mH)

Table 2: Performance of 8/6 SRM operating with fixed switching angles

$T_{e(max)}$	$T_{e(min)}$	$T_{e(avg)}$	TRF
16.12	6.285	12.291	0.8002

$$\frac{1}{2}i^2\frac{dL(\theta,i)}{d\theta}-T_l = J\frac{\omega_m}{dt}+B\omega_m \qquad (4)$$

Where:

V = The applied phase voltage
R_s = The phase resistance
L = The phase inductance
ω_m = The motor angular speed
θ = The rotor position
I = The phase current
T_e = The developed electromagnetic torque
T_l = The load torque

Figure 2 shows the performance of SRM Model using fixed switching angles. Table 2 shows the model performance has been measured using Torque Ripple Factor (TRF) calculated by Eq. 5:

$$TRF = \frac{T_{e(max)}-T_{e(min)}}{T_{e(avg)}}\% \qquad (5)$$

High TRF in Table 2 shows poor performance of the model, so, it is required to use a suitable controller to achieve good control and performance with the proper choice of gains.

Modeling of PI-PSO controller: In this subsection, the PI-PSO controller is proposed. The method of tuning the parameters of PI controller (K_p and K_i) by the Particle Swarm Optimization (PSO) is briefly reviewed (El-Wakeel *et al*., 2013, 2015; Saha and Panda, 2017). In the PSO algorithm a population of particles is put into the d-dimensional search space with randomly chosen velocities and positions knowing their best values, so far, (pbest) and the position in the d-dimensional space. The velocity of each particle is adjusted according to its own flying experience and the other particle's flying experience as follows (Eslami *et al*., 2012; Ilic-Spong *et al*., 1987):

$$v_i^{k+1} = wv_i^{k+1}+c_1 rand_{1i}\times\left(pbest_i-s_i^k\right)+c_2 rand_{2i}\times\left(gbest-s_i^k\right) \quad (6)$$

Where:

V_i^k = The current velocity of particle
I = At iteration k
V_i^{k+1} = The updated velocity of particle I
w = The inertia weight
c_1, c_2 = Two acceleration positive PSO constants
s_i^k = The current position of particle i at iteration k
$rand_{1i}$, $rand_{2i}$ = Random numbers between 0 and 1
$pbest_i$ = The best position of particle I
gbest = The global best position of the group, so far

$$S_i^{k+1} = S_i^k + V_i^{k+1} \quad (7)$$

Where:

V_i^{k+1} = The new position
S_i^k = Can be modified using the present position
V_i^{k+1} = Updated velocity

The positive constants c_1 and c_2 are both set to 2. The inertia weight W is set as a decreasing linear function with the itration number from 0.9-0.4. This large value of inertia weight at the beginning enhances the PSO global searching ability while the small inertia weight near the end of ther run improves its local search ability. The fitness function value is calculated for each particle. If the value is better than the current pbest of the particle, the pbest value is replaced by the current value. If the best value of pbest is better than the current gbest, the gbest is replaced by the best value and the particle number with the best value is stored. The operation is continued until the current iteration number reaches the predetermined maximum iteration number.

Table 3: PSO parameters

Variables	Values
Population	100.0
Number of iterations	020.0
w_{max}	000.9
w_{min}	000.4
c_1	002.0
c_2	002.0

The PSO algorithm has been run for 20 independent trials with different settings until the solutions are very close to each other. According to the trials, the PSO parameters are summarized in Table 3.

Modeling of PI-FA controller: In this subsection, the PI-FA controller is proposed (Abdel-Hamed *et al*., 2016). The FA is a population-based optimization algorithm that has many similarities to other population-based algorithms such as PSO and BFO (Mohammadi *et al*., 2014). The FA is based on the following three ideas (Bendjeghaba, 2014) all fireflies are supposed to be unisex and will move toward more attractive and brighter fireflies regardless their sex the firefly with less brightness is attracted in the direction of the firefly with more brightness and it is the brightness of each firefly that determines its attractiveness (light intensity) and in the case that no firefly with more brightness is recognized, the firefly will move randomly in the search space. In the optimization algorithm, fireflies use two main procedures: attractiveness and movement which are described in what follows.

Attractiveness of fireflies: The space between two fireflies (r) rises, less light can be observed by the fireflies (less attractiveness). For simulation of firefly behavior any monotonically minimizing function as in Eq. 8 (Abdel-Hamed *et al*., 2016).

$$\beta(r) = \beta_0.\exp\left(-\gamma.r^m\right) \qquad m>1 \quad (8)$$

Where:

r = The distance between different two fireflies in search space
γ = The absorption coefficient
β_0 = The initial attractiveness when the distance r = 0
I = The distance r between firefly vectors
j = The optimization search space at positions
x_i and x_j = Which is like to the distance between the fireflies in the air can be defined as shown in Eq. 9 (Abdel-Hamed *et al*., 2016)

$$r_{ij} = \| x_i - x_j \| = \sqrt{\sum_{l=1}^{d} \left(x_{i,l} - x_{i,l} \right)^2} \quad (9)$$

Where:

$x_{i,l}$ = The component of the spatial coordinates
x_i = The dimension of the investigated optimization problem

Movement of fireflies: The movement of the ith firefly (less light intensity) toward the jth firefly (more light intensity) is mathematically formulated as in Eq. 10:

$$x_i = x_i + \beta_o . \exp\left(-\gamma . r^m\right) . \left(x_j - x_i\right) + \alpha . \left(\text{rand} - 0.5\right) \quad (10)$$

The first section of Eq. 10 is the current location of the ith firefly, the second section simulates the brightness of the jth firefly realized by the jth firefly and the third section agrees the ith firefly to move randomly in the whole search space when no brighter firefly is observable around it.

Random selection parameter of factor α is determined through a problem of advantage while a random number produced uniformly spread in the space (0.0, 1.0). According to current works it is shown that the optimal of the two variables β_{oi} and γ depends on the characteristics of the inspected problem.

Objective function: The objective function to be decreased has been taken into consideration as a complete performance index during the simulation period. Equation 11 explains the IAE fitness functions used in the optimization. Eq. 12 shows the subjected performance index to be minimized with optimization.

$$IAE = \int_0^{T_{max}} |\Delta V| dt \quad (11)$$

$$WGAM = a_1 \int_0^{T_{max}} |\Delta V^2| dt + a_2 \int_0^{T_{max}} \left[\left(Q_{comp} - Q_{ref} \right)^2 \right] dt \quad (12)$$

Where:

ΔV = Voltage deviation
$(Q_{comp}-Q_{ref})$ = The difference between the value of reacive power of compensator and the reference reactive power from grid
a_1 and a_2 = Positive constants (weighting factor) with values selected according to their importance priority between (0, 1) such that $a_1 = 0.6$ and $a_2 = 0.4$

In this study, $c_1 = c_2 = 0.5$ and the basic FA parameters used here in are given in Table 4.

Table 4: FA parameters

Parameters of FFA	Values
Number of fireflies (N)	30
Number of iterations (Ng)	25
Randomness (α)	0.7
Initial attractiveness (β_o)	0.4
Aborption coefficient (γ)	1

Torque Sharing Functions (TSF): The TSF is a torque control method which applies premeasured nonlinear torque characteristics and simply uses a torque sharing curve for constant torque production. TSF is a simple but powerful and popular method as it simply divides the torque by a sharing curve in which the phase torque can be assigned to each phase current that can be used for constant torque generation. The current ripple should be kept small enough due to the relationship between the phase torque and the square of the phase current (Jin-Woo, 2011).

Figure 3 shows a torque control block diagram with TSF method of a 6/4 SRM. The input torque reference is divided into three-phase torque commands based on the rotor position. The torque commands of each phase are changed to current command signal in the "Torque-to-Current" block according to rotor position. The output torque is determined by the inductance slope and phase current. The inductance slope depends on the rotor position. So, the reference current of each phase is determined by the target torque and rotor position. The switching rule develops an active switching signal of asymmetric converter based on current error and hysteresis switching tables (Jin-Woo, 2011).

In the overlap region of inductances, the two-phase currents produce the output torque together. Simple torque sharing curves are applied for constant torque generation in the commutation region such as, linear and cosine function (Jin-Woo, 2011). Figure 4 shows the linear, cosine and cubic TSF curves. It is clear that in the activation regions, the TSF is identical, however, it is different in the commutation regions.

The linear TSF has constant slope of torque in commutation region. This method is simple but it is quite difficult to generate the linear torque slope in the commutation region because of the non linear inductance characteristics (Jin-Woo, 2011; Schramm *et al*., 1992; Dowlatshahi *et al*., 2014).

The cosine function is relatively simple and it is identical to the nonlinear inductance characteristics. However, the nonlinear characteristics of SRM are very complicated. So, the cosine TSF is not sufficient in the aspect of torque ripple and efficiency (Jin-Woo, 2011; Dowlatshahi *et al*., 2014; Hussain and Ehsani, 1996; Saha and Panda, 2017).

The cubic TSF was proposed in a trial to generate a smooth function. The torque produced by the phases during phase commutation changes nonlinearly with the rotor position. This nonlinearity has the form of a cubic polynomial (Sahoo *et al*., 2004, 2005).

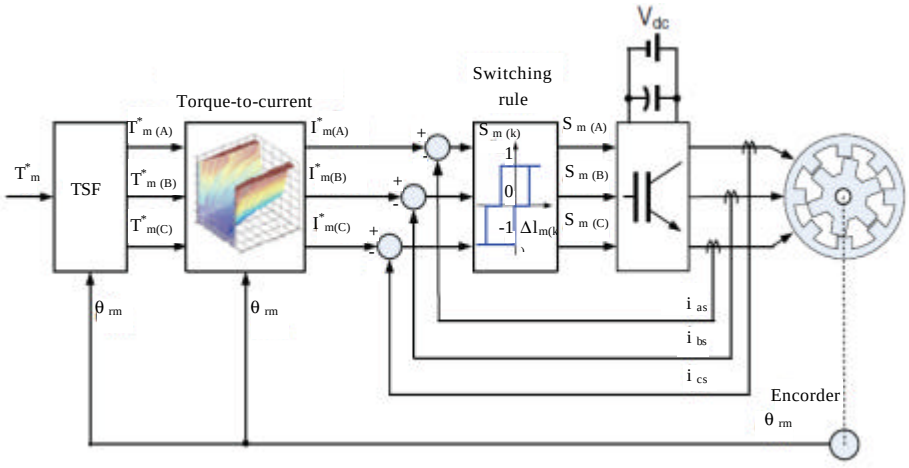

Fig. 3: Torque control block diagram with TSF method

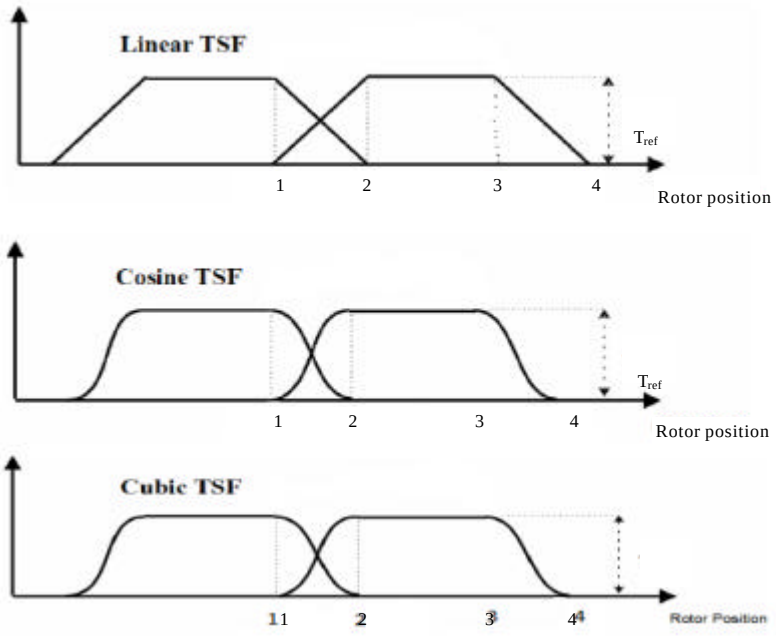

Fig. 4: Linear, cosine and cubic TSF curves

For torque ripples reduction and efficiency improvement a nonlinear current distribution technique is used by the TSF in commutation regions. The TSF can be easily obtained by the current coordinates of each rotor position.

In the commutation region, the total torque reference T^*_m is distributed between two phase torque references $T^*_{m(k)}$ and $T^*_{m(k-1)}$ as follows (Bendjeghaba, 2014; Jin-Woo, 2011; Dowlatshahi *et al.*, 2014):

$$^{*}_{m} \quad ^{*}_{m(k)} \quad ^{*}_{m(k-1)} \tag{13}$$

$$\tag{14}$$

$$T^*_{m(k-1)} = T^*_m \cdot f^*_{k-1}(\theta) \tag{15}$$

$$f^*_k(\theta)+f^*_{k-1}(\theta)=1 \tag{16}$$

$$f^*_{k+1}(\theta)=0 \tag{17}$$

The linear TSF of each phase can be obtained as follows: (Jin-Woo, 2011; Schramm *et al.*, 1992; Dowlatshahi *et al.*, 2014):

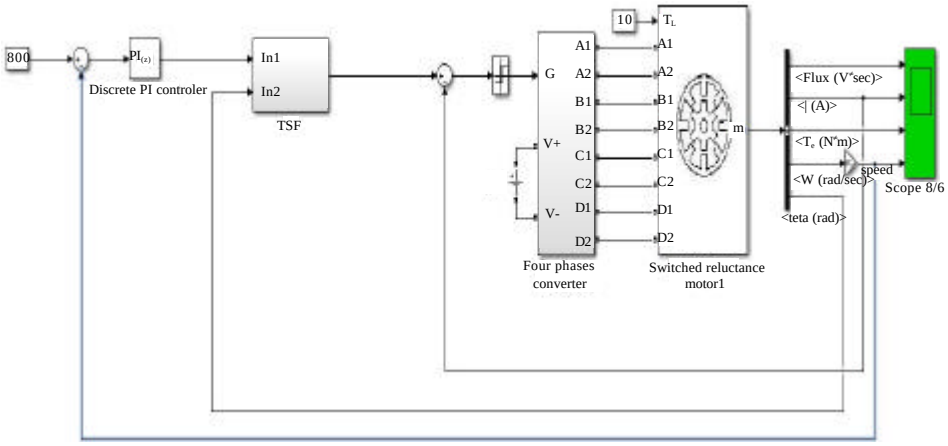

Fig. 5: Simulink Model of 8/6 SRM with TSF/PI controller

$$f_{linear}=\begin{cases}\frac{\theta-\theta_1}{\theta_2-\theta_1} & ,\ \theta_1\le\theta<\theta_2\\ 1 & ,\ \theta_2\le\theta<\theta_3\\ 1-\frac{(\theta-\theta_4+\theta_2-\theta_1)}{(\theta_2-\theta_1)} & ,\ \theta_3\le\theta<\theta_4\end{cases} \quad (18)$$

The cosine TSF of each phase can be defined as follows: (Jin-Woo, 2011; Dowlatshahi *et al*., 2014; Hussain and Ehsani, 1996; Saad *et al*., 2017; Vujicic, 2012):

$$f_{Cosine}=\begin{cases}0.5-0.5\cos 4(\theta-\theta_1) & ,\ \theta_1\le\theta<\theta_3\\ 1 & ,\ \theta_2\le\theta<\theta_3\\ 0.5+0.5\cos 4(\theta-\theta_3) & ,\ \theta_3\le\theta<\theta_4\end{cases} \quad (19)$$

And the cubic TSF of each phase can be obtained as follows:(Sahoo *et al*., 2004, 2005):

$$f_{cubic}=\begin{cases}3\left(\frac{\theta-\theta_1}{\theta_1-\theta_2}\right)^2-2\left(\frac{\theta-\theta_1}{\theta_1-\theta_2}\right)^3 & ,\theta_1\le\theta<\theta_2\\ 1 & ,\theta_2\le\theta<\theta_3\\ 1-\left[\left(\frac{(\theta-\theta_4+\theta_1-\theta_2)}{(\theta_1-\theta_2)}\right)^2-2\left(\frac{(\theta-\theta_4+\theta_1-\theta_2)}{(\theta_1-\theta_2)}\right)^3\right] & ,\theta_3\le\theta<\theta_4\end{cases}$$

Where:

f = The sharing function
θ = The rotor position
k and k-1 = The outgoing and incoming phases, respectively

RESULTS AND DISCUSSION

In order to achieve better performance and minimum torque ripples, a PI controller shown in Fig. 5 with three types of TSFs (linear, cosine and cubic) discussed earlier in Eq. 3 will be used for speed control and torque ripple minimization of SRM. The gains of PI controller (K_p and K_i) will be determined using the following tuning methods:

- Manual tuning
- Particle Swarm Optimization (PSO) as described in Eq. 2
- Firefly Algorithm (FA) as described in Eq. 2

The PI controller is used for the speed control of SRM. Controller gains (K_p and K_i) are determined based on minimum torque error developed. Gains of each tuning method are shown in Table 5.

All three types of TSF are combined with the three PI controllers forming nine different control systems. TRF for the developed torque of each system running at reference speed ω_{ref} = 800 rpm and a load T_L = 10 N.m is measured. The torque curves for linear, cosine and cubic TSF systems are shown in Fig. 6-8.

By examining the TRF and the developed torque performance curves of the systems mentioned above it can be concluded that behaviour of the 7.5 kW 8/6 SRM using Cubic TSF/PI-FA gives the best performance and achieves a minimum TRF of 0.02031 as illustrated in Table 6 and Fig. 9.

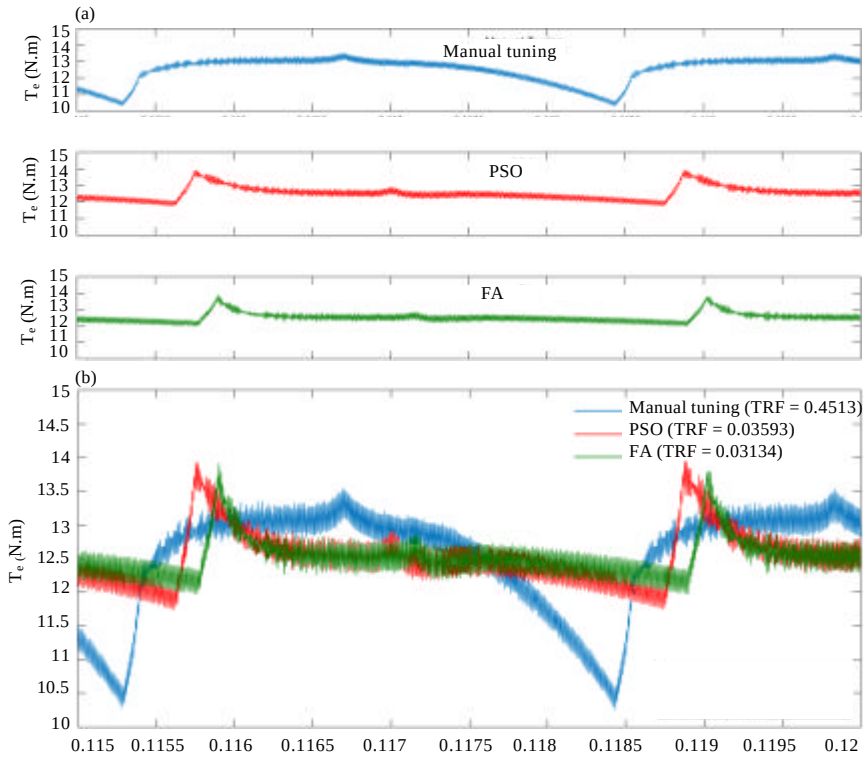

Fig. 6: Performance of 8/6 SRM using linear TSF with three

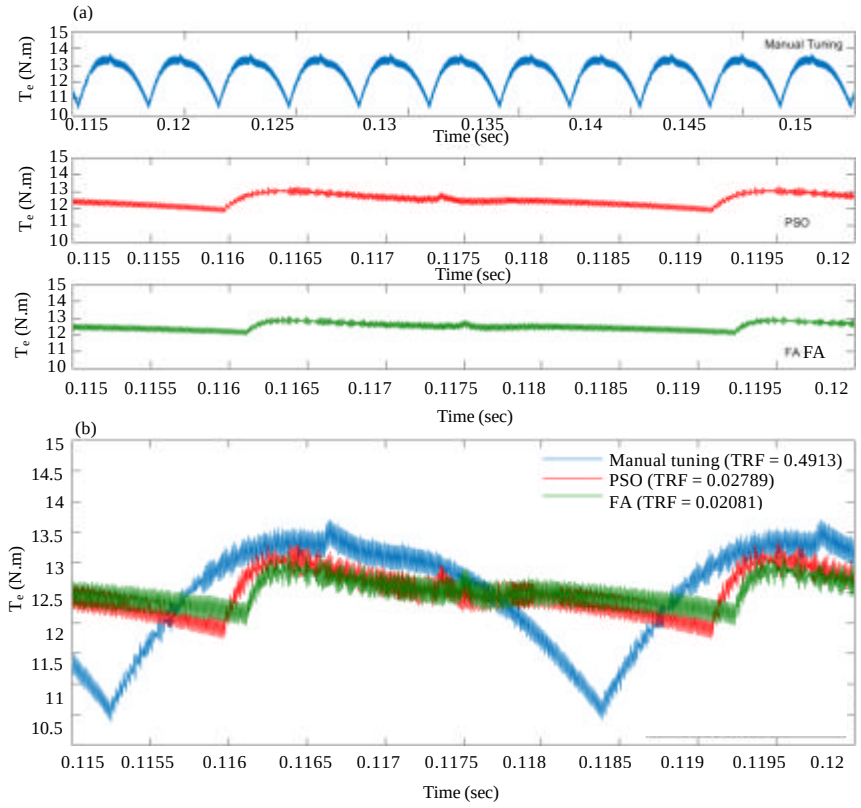

Fig. 7: Performance of 8/6 SRM using cosine TSF with three optimization techniques

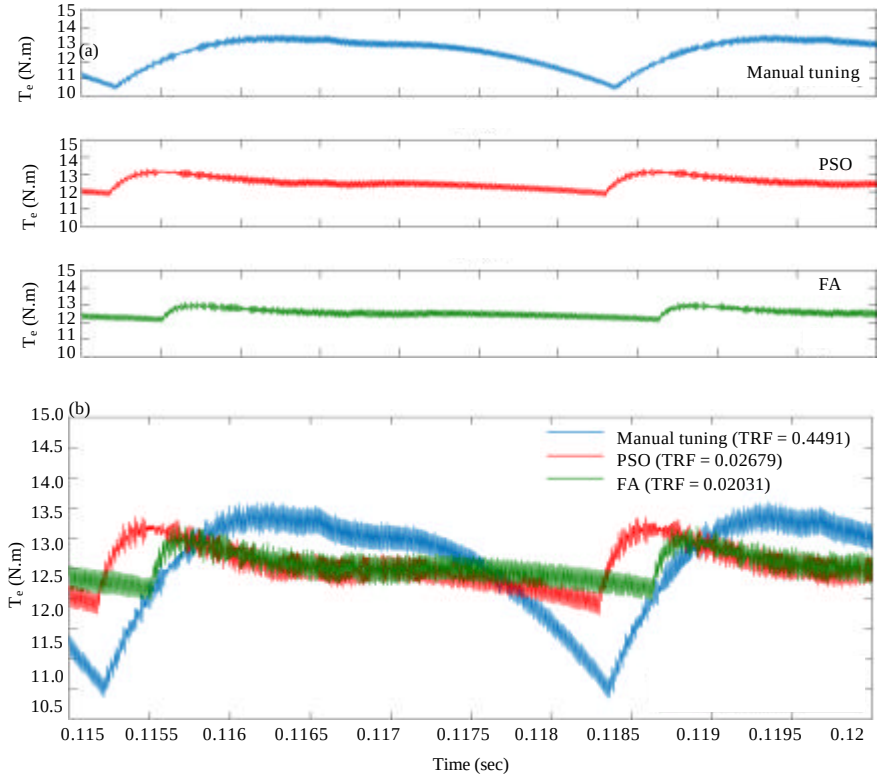

Fig. 8: Performance of 8/6 SRM using cubic TSF with three optimization techniques

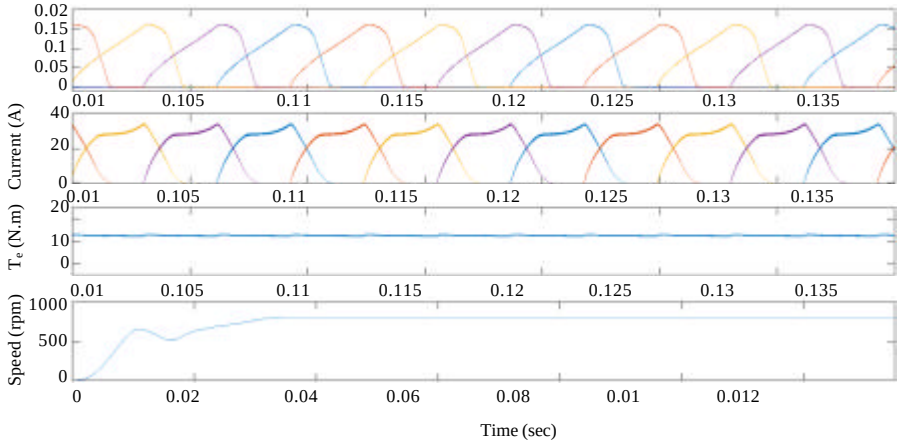

Fig. 9: Performance of 8/6 SRM using cubic TSF and FA gains

Table 5: Gains of tuning methods for PI controller

Methods	Manual tuning	PSO	FA
K_p	0.2	10.889	19.994
K_i	0.002	0.987	0.3719

Table 6: TRF values for nine closed loop TSF/PI controlled systems

TSF/PI	Manual tuning	PSO	FA
Linear	0.4513	0.03593	0.03134
Cosine	0.4913	0.02789	0.02081
Cubic	0.4491	0.02679	0.02031

CONCLUSION

This study deals with improving SRM performance, especially, torque ripples reduction by using an optimal speed controller. The poor performance of SRM under single phase control with fixed switching angles was also discussed. In this study, gains of PI speed controller are optimized for achieving the best developed current and torque profiles and the least Torque Ripple Factor (TRF).

A Torque Sharing Function (TSF) is then used such that the phase torque is divided and assigned to each phase current based on the rotor position for constant torque generation. MATLAB/Simulink tool was used for simulating and studying the performance of a 7.5 kW 8/6 SRM. A comparative study between nine PI controlled systems with three optimization techniques (i.e., manual tuning, PSO and FA) and three types of TSFs (i.e., linear, cosine and cubic) based on minimum developed torque ripple at reference speed ω_{ref} = 800 rpm and a load T_L = 10 N.m has been also presented. Results show that cubic TSF/PI-FA gives the best performance and achieves the minimum TRF for this type of SRM.

REFERENCES

Abdel-Hamed, A.M., A.E.E.K.M. Ellissy, A.S. El-Wakeel and A.Y. Abdelaziz, 2016. Optimized control scheme for frequency/power regulation of microgrid for fault tolerant operation. Electr. Power Compon. Syst., 44: 1429-1440.

Bendjeghaba, O., 2014. Continuous firefly algorithm for optimal tuning of PID controller in AVR system. J. Electr. Eng., 65: 44-49.

Dowlatshahi, M., S.M. Saghaiannejad, J.W. Ahn and M. Moallem, 2014. Minimization of torque-ripple in switched reluctance motors over wide speed range. J. Electr. Eng. Technol., 9: 478-488.

El-Wakeel, A., 2003. Design optimisation for fault tolerant switched reluctance motors. Ph.D Thesis, University of Manchester Institute of Science and Technology, Manchester, England, UK.

El-Wakeel, A.S., A.E.E.K.M. Ellissy and A.M. Abdel-Hamed, 2015. A hybrid bacterial foraging-particle swarm optimization technique for optimal tuning of proportional-integral-derivative controller of a permanent magnet brushless DC motor. Electr. Power Compon. Syst., 43: 309-319.

El-Wakeel, A.S., F. Hassan, A. Kamel and A. Abdel-Hamed, 2013. Optimum tuning of PID controller for a permanent magnet brushless DC motor. Int. J. Electr. Eng. Technol., 4: 120-135.

Eslami, M., H. Shareef, M. Khajehzadeh and A. Mohamed, 2012. A survey of the state of the art in particle swarm optimization. Res. J. Appl. Sci. Eng. Technol., 4: 1181-1197.

Hussain, I. and M. Ehsani, 1996. Torque Ripple minimization in switched reluctance motor drives by PWM current control. IEEE Trans. Power Elect., 11: 83-88.

Ilic-Spong, M., R. Marino, S. Peresada and D. Taylor, 1987. Feedback linearizing control of switched reluctance motors. IEEE. Trans. Autom. Control, 32: 371-379.

Jin-Woo, A., 2011. Switched Reluctance Motor. In: Torque Control, Lamchich, M.T. (Ed.). InTech Publisher, London, England, UK., pp: 201-252.

Krishnan, R., 2001. Switched Reluctance Motor Drives, Modeling, Simulation, Analysis, Design and Applications. 1st Edn., CRC Press LLC, UK.

Miller, T.J.E., 2001. Electronic Control of Switched Reluctance Machines. Newness Publisher, Boston, Massachusetts, USA., ISBN:0-7506-50737, Pages: 272.

Mohammadi, S., S. Soleymani and B. Mozafari, 2014. Scenario-based stochastic operation management of microgrid including wind, photovoltaic, micro-turbine, fuel cell and energy storage devices. Intl. J. Electr. Power Energy Syst., 54: 525-535.

Saad, N.H., A.A. El-Sattar and M.E. Metally, 2017. Artificial neural controller for torque ripple control and maximum power extraction for wind system driven by switched reluctance generator. Ain Shams Eng. J., 1: 1-10.

Saha, N. and S. Panda, 2017. Speed control with torque ripple reduction of switched reluctance motor by Hybrid many optimizing liaison gravitational search technique. Eng. Sci. Technol. Intl. J., 20: 909-921.

Sahoo, S.K., S.K. Panda and J.X. Xu, 2004. Iterative learning-based high-performance current controller for switched reluctance motors. IEEE. Trans. Energy Convers., 19: 491-498.

Sahoo, S.K., S.K. Panda and J.X. Xu, 2005. Indirect torque control of switched reluctance motors using iterative learning control. IEEE. Trans. Power Electron., 20: 200-208.

Schramm, D., B.W. Williams and T.C. Green, 1992. Torque ripple reduction of switched reluctance motors by phase current optimal profiling. Proceedings of the 23rd Annual IEEE Power Electronics Specialists Conference, Jun 29-Jul 3, Toledo, pp: 857-860.

Torrey, D.A., X.M. Niu and E.J. Unkauf, 1995. Analytical modelling of variable-reluctance machine magnetisation characteristics. IEE. Proc. Electr. Power Appl., 142: 14-22.

Vujicic, V.P., 2012. Minimization of torque ripple and copper losses in switched reluctance drive. IEEE. Trans. Power Electron., 27: 388-399.